



Pergamon

Acta mater. 49 (2001) 1599–1605



www.elsevier.com/locate/actamat

DISLOCATION EVOLUTION IN EPITAXIAL MULTILAYERS AND GRADED COMPOSITION BUFFERS

T. C. WANG^{1†}, Y. W. ZHANG² and S. J. CHUA²

¹LNM, Institute of Mechanics, Chinese Academy of Science, Beijing 100080, People's Republic of China and ²Institute of Materials Research and Engineering, 3 Research Link, Singapore 117602

(Received 14 November 2000; received in revised form 17 January 2001; accepted 17 January 2001)

Abstract—This paper presents models to describe the dislocation dynamics of strain relaxation in an epitaxial uniform layer, epitaxial multilayers and graded composition buffers. A set of new evolution equations for nucleation rate and annihilation rate of threading dislocations is developed. The dislocation interactions are incorporated into the kinetics process by introducing a resistance term, which depends only on plastic strain. Both threading dislocation nucleation and threading dislocation annihilation are characterized. The new evolution equations combined with other evolution equations for the plastic strain rate, the mean velocity and the dislocation density rate of the threading dislocations are tested on $\text{Ge}_x\text{Si}_{1-x}/\text{Si}(100)$ heterostructures, including epitaxial multilayers and graded composition buffers. It is shown that the evolution equations successfully predict a wide range of experimental results of strain relaxation and threading dislocation evolution in the materials system. Meanwhile, the simulation results clearly signify that the threading dislocation annihilation plays a vital role in the reduction of threading dislocation density. © 2001 Acta Materialia Inc. Published by Elsevier Science Ltd. All rights reserved.

Keywords: Epitaxial multilayers; Dislocations

1. INTRODUCTION

During the past 25 years a great deal of experimental research has focused on strain relaxation via the creation of misfit dislocations in lattice-mismatched epitaxial thin films [1, 2]. Although much progress has been made—for example, by controlling dislocation dynamics and surface roughness [3, 4], relaxed epitaxial layers, especially composition graded buffer layers with relatively high quality, have recently been grown—the mechanics behind the strain relaxation, however, is not well understood.

Recently there has been increasing interest in epitaxial graded composition buffers, which are believed to be promising materials for high-performance optoelectronic devices. In the growth of graded buffers, threading dislocations are concomitantly generated with misfit dislocations. Since the threading dislocations are deleterious to the performance of optoelectronic and microelectronic devices, reducing the threading dislocation density therefore becomes an important task. Several theoretical efforts have been made to understand the mechanics and physics under-

lying threading dislocation reduction. The first kinetic description of strain relaxation by misfit dislocations was given by Dodson and Tsao [5]. They proposed a phenomenological model to describe the plastic strain rate. Hull *et al.* [6] developed a kinetic model to simulate the relaxation process. Houghton [7] proposed a set of evolution equations to interconnect the nucleation and propagation of threading dislocations and the formation of misfit dislocations. Subsequent models [3, 8] have been proposed along a similar line. Fitzgerald *et al.* [9] clearly revealed that dislocation annihilation plays an essential role in the reduction of threading dislocation densities, and that surface control can be effective in the reduction of threading dislocation densities. Romanov *et al.* [10] proposed a model for threading dislocation reduction by introducing an intentionally strained layer. Three types of dislocation were considered in their model.

It is clear that a sound model of strain relaxation should include the major elements of the strain relaxation processes: nucleation, propagation, interaction and multiplication of dislocations. In this paper, we present models to describe the dislocation dynamics of strain relaxation in an epitaxial uniform layer, epitaxial multilayers and graded composition buffers by including these elements. A set of new evolution equations for nucleation rate and annihilation rate of threading dislocations is developed. The dislocation interactions are incorporated into the kinetics process.

† To whom all correspondence should be addressed. Tel.: +86 10 6255 4160; Fax: +86 10 6256 1284.

E-mail address: tcwang@cc5.imech.ac.cn (T. C. Wang)

2. DISLOCATION DYNAMICS IN SINGLE EPITAXIAL LAYER

In order to get a clear picture of the kinetic process of strain relaxation, we start working on a uniform single epitaxial layer deposited on a thick substrate. The relaxed plastic strain rate can be expressed by the equation [2, 9]

$$\dot{\epsilon}_p = \rho b_1 v / 2, \quad (1)$$

where ρ is the mobile threading dislocation density, b_1 is the dislocation component parallel to the interface and perpendicular to corresponding misfit dislocation lines, and v is the mean velocity of the threading dislocation. Equation (1) can trace back to the classical Orowan equation [11].

The evolution equations for the mean velocity and density rate of the threading dislocations can be expressed as [6, 7, 9]

$$v = v_0 \left(\frac{\tau_{\text{exc}} - \tau_R}{\mu} \right)^m \exp\left(-\frac{Q_v}{kT}\right) \quad (2)$$

and

$$\dot{\rho} = \dot{\rho}_{\text{nucl}} - \dot{\rho}_{\text{annih}}, \quad (3)$$

where μ is the shear modulus of the epitaxial layer, Q_v is the activation energy for the velocity of the threading dislocations, k is Boltzmann's constant, T is the absolute temperature, $\dot{\rho}_{\text{nucl}}$ is the nucleation rate of the threading dislocations, and $\dot{\rho}_{\text{annih}}$ is the annihilation rate of the threading dislocations.

The new evolution equations for the nucleation rate $\dot{\rho}_{\text{nucl}}$ and the annihilation rate $\dot{\rho}_{\text{annih}}$ of the threading dislocations take the forms

$$\dot{\rho}_{\text{nucl}} = \xi_0 \left(\frac{\tau - \tau_0 - \tau_R}{\mu} \right)^n \exp\left(-\frac{Q_p}{kT}\right) \quad (4)$$

and

$$\dot{\rho}_{\text{annih}} = \rho v / p, \quad (5)$$

where Q_p is the activation energy for the nucleation rate of the threading dislocations, p is the misfit dislocation spacing, τ is the coherency stress produced by elastic misfit strain, τ_0 is the threshold stress for threading dislocation nucleation, and τ_{exc} is the excess stress. τ and τ_{exc} can be expressed as [1, 2]

$$\tau = c\mu(\epsilon_0 - \epsilon_p) \quad (6a)$$

and

$$\tau_{\text{exc}} = c\mu \left\{ (\epsilon_0 - \epsilon_p) - \frac{\Gamma b}{h} \ln(2h/b) \right\}, \quad (6b)$$

where $c = 2(1 + \nu)/(1 - \nu)$, ν is the Poisson's ratio, ϵ_0 is the mismatch strain between the epitaxial layer and substrate, ϵ_p is the relaxed plastic strain, h is the thickness of the epitaxial layer and Γ is a material constant,

$$\Gamma = \frac{(1 - \nu \cos \theta)}{4\pi(1 + \nu)}, \quad (7)$$

where θ is the angle between the misfit dislocation line and the Burgers vector. τ_R is the resistance to the threading dislocation gliding arising from dislocation interactions and surface roughness, which can be expressed as

$$\tau_R = c\mu H(\epsilon_p) = c\mu\alpha \left(\frac{\epsilon_p}{\epsilon_L} \right)^\beta \left[1 - \tanh\left(\frac{\gamma\epsilon_p}{\epsilon_L}\right) \right], \quad (8)$$

where ϵ_L is the maximum misfit between the epitaxial film and the thick substrate. For the $\text{Ge}_x\text{Si}_{1-x}/\text{Si}$ system, $\epsilon_L = 0.0418$ (at $x = 1$). The parameters α , β and γ are material constants. Usually the function $H(\epsilon_p)$ is called the work hardening function. The power-law hardening function $\alpha(\epsilon_p/\epsilon_L)^\beta$ is well known in plasticity theory. The term $[1 - \tanh(\gamma\epsilon_p/\epsilon_L)]$ prevents the material behaviour from being hardening too quickly. When $\gamma = 0$, the epitaxial film becomes a pure power-law hardening material.

The present model assumes that dislocation multiplication during glide plays a relatively minor role compared with dislocation nucleation and that the threading dislocations can flow unimpeded through the structure. Partial threading dislocations may be pile-ups at the surface or in the structure, but this does not stop the mobile threading dislocations moving. Since the threading dislocations nucleate at the surface, the tension stress associated with the energy required to create a new misfit dislocation segment has no direct effect on threading dislocation nucleation. The surface morphology plays a vital role in the kinetic process of threading dislocation nucleation and has a significant effect on the threshold stress τ_0 . We should emphasize that equation (4) is only suitable for the case of $\nu > 0$, otherwise $\dot{\rho}_{\text{nucl}}$ should be equal to zero.

The kinetic process leads to a more or less regular array of parallel misfit dislocations on the interface. For a cubic crystal with a [110] interface, such arrays commonly form along both [110] and $[1\bar{1}0]$ directions in the interface. If the mean spacing of the misfit dislocations in an array is denoted by p , then one can find two perpendicular periodic arrays of misfit dislocations, which form a periodic array of rectangular cells. One can choose one cell as a typical sample for consideration. For an ideal periodic array of rectangular cells one can easily obtain equation (5). But in reality, nucleation sources of threading dislocations are randomly distributed. The nucleation sources in different cells have different spatial distributions. Obviously, a complete annihilation can never be realized, hence equation (5) should be modified as

$$\dot{\rho}_{\text{annih}} = \eta_0 \rho v / p, \quad (9)$$

where the coefficient η_0 is the effective factor of annihilation reactions of mobile threading dislocations with other threading dislocations. This factor depends on many complex factors such as fabrication technology, surface morphology and composition structure. There is no predictable formula to estimate its value. Here we only suggest an empirical formula

$$\eta_0 = \begin{cases} 1, & p^2 \rho \geq 10 \\ \frac{p^2 \rho}{10}, & p^2 \rho \leq 10 \end{cases} \quad (10)$$

The new evolution equations are tested on the $\text{Ge}_x\text{Si}_{1-x}/\text{Si}$ material system. The material parameters m , n , Q_v and Q_ρ were measured experimentally by Hull *et al.* [6] and Houghton [7]. In this paper we take the following data [6, 7]: $m = 2.0$, $n = 2.5$, $Q_v = 1.1$ eV and $Q_\rho = 2.2$ eV. The materials parameters α , β and γ can be evaluated from annealing experiments. Figure 1 shows the experimental results given by Hull *et al.* [6] for the growth–annealing of $x = 0.25$ structures at a growth rate of 0.3 nm s⁻¹. Experimental data were given for growth at 550°C plus *in situ* annealing at 800°C for 10 min in the molecular beam epitaxy (MBE) chamber in terms of the average measured misfit dislocation spacing, p , versus epitaxial layer thickness, h . After 10 min annealing at 800°C the material system should arrive at an equilibrium state. The equilibrium relaxed plastic strain can be obtained from equations (2), (6) and (8) by setting $\tau_{\text{exc}} - \tau_{\text{R}} = 0$,

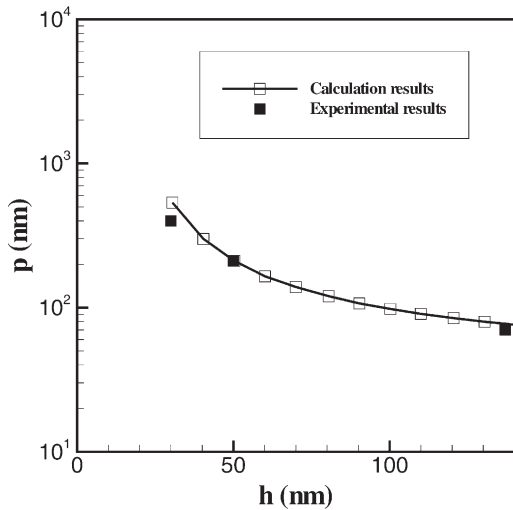


Fig. 1. Comparison of experiment and present modelling for growth–annealing of $\text{Ge}_x\text{Si}_{1-x}/\text{Si}(100)$ structure with $x = 0.25$. Experimental data (filled points) were given by Hull *et al.* [6] for growth at 550°C plus *in situ* anneal at 800°C for 10 min in the MBE chamber, for the average measured misfit dislocation spacing, p , versus epitaxial layer thickness, h . The growth rate was 0.3 nm s⁻¹. All unfilled points are the present simulation results.

$$\varepsilon_p = \varepsilon_0 - \frac{\Gamma b}{h} \ln(2h/b) - H(\varepsilon_p). \quad (11)$$

For the $\text{Ge}_x\text{Si}_{1-x}/\text{Si}(100)$ material system, $v = 0.22$ and $b = 0.384$ nm. From the three experimental data points corresponding to growth at 550°C followed by a 10 min anneal in Fig. 1, one can easily obtain the parameters α , β and γ . We have $\alpha = 0.0166$, $\beta = 0.198$ and $\gamma = 5.0$. At equilibrium state the nucleation rate $\dot{\rho}_{\text{nuc}}$ vanishes. Hence we have

$$\tau - \tau_0 - \tau_{\text{R}} \leq 0. \quad (12)$$

Equation (12) can be rewritten as

$$\tau_0 \geq c\mu[\varepsilon_0 - \varepsilon_p - H(\varepsilon_p)] = c\mu \frac{\Gamma b}{h} \ln(2h/b). \quad (13)$$

If we assume that the equality of equation (13) holds at the data point of $h = 35$ nm, then we obtain $\tau_0 = c\mu\varepsilon_0$, $\varepsilon_0 = 0.003488$ (at the beginning we chose the experimental data point of $h = 30$ nm in Fig. 1, but after testing we found that the corresponding result of τ_0 seems a little higher).

In order to obtain the parameters v_0 and ξ_0 , let us look at the experimental results of Hull *et al.* [6] obtained by thermal annealing for 4 min a 35 nm thick $\text{Ge}_x\text{Si}_{1-x}/\text{Si}(100)$ layer with $x = 0.25$ after growth at each temperature. Figure 2(a) shows the average misfit dislocation spacing, p , and Fig. 2(b) shows the threading dislocation density, ρ . Only by using two experimental data points at 550°C , one can easily get the parameters v_0 and ξ_0 . They are $v_0 = 0.32 \times 10^{14}$ nm s⁻¹ and $\xi_0 = 0.55 \times 10^{10}$ nm⁻² s⁻¹. All together only five experimental data points are used in determining the materials parameters α , β , γ , v_0 and ξ_0 .

Now all material parameters are known, one can simulate the kinetic process for the materials system $\text{Ge}_x\text{Si}_{1-x}/\text{Si}(100)$. The present model's results for growth and growth–annealing of the $x = 0.25$ structure are also shown in Fig. 1. The three experimental data points corresponding to growth at 550°C plus annealing at 800°C for 10 min are a little lower than the theoretical curve. This means that, when the thickness is smaller than 50 nm, the simulated evolution process has not yet arrived at the real equilibrium state, and a longer annealing time is needed for the system to arrive at real equilibrium. The experimental and present simulation results for thermal annealing are also shown in Fig. 2. It is apparent that the theoretical results agree well with the experimental data.

The critical thickness theory states that the final elastic strain is dependent only on the epitaxial layer thickness, no matter what the value of ε_0 . This is in total contrast with the experimental observation given by Bean *et al.* [12, 13], which clearly shows that the final elastic strains do vary remarkably with the initial mismatch. A comparison of the experimental results

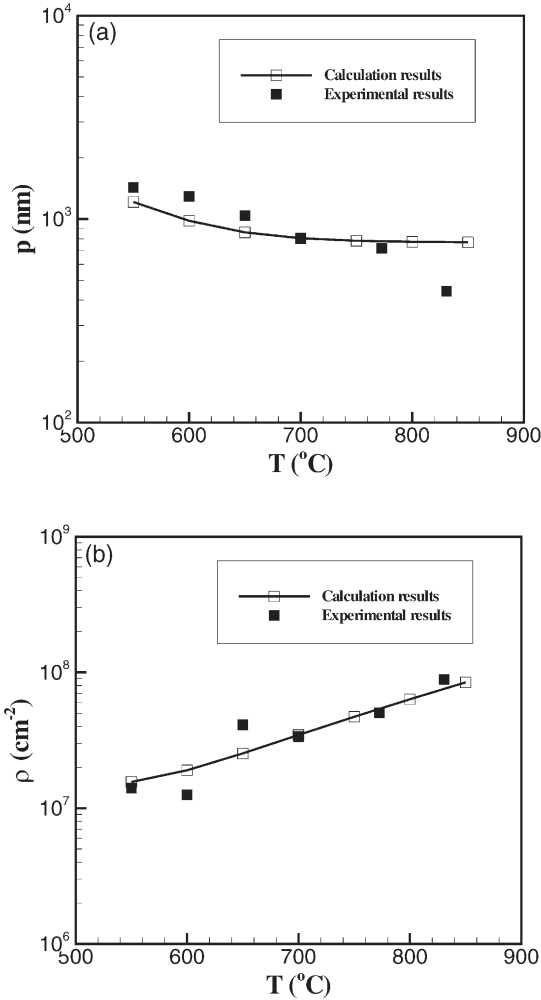


Fig. 2. Comparison of experiment and present modelling for growth and growth-annealing of a 35 nm thick $\text{Ge}_x\text{Si}_{1-x}/\text{Si}(100)$ structure with $x = 0.25$. Experimental data (filled points) were given by Hull *et al.* [6] for growth and 4 min annealing at each temperature. The growth rate was 0.3 nm s^{-1} . (a) Average misfit dislocation spacing, p ; (b) threading dislocation density, ρ . All unfilled points are the present calculation results.

and the present simulation results for final elastic strain versus initial mismatch strain following growth of the $\text{Ge}_x\text{Si}_{1-x}/\text{Si}(100)$ at 550°C is given in Fig. 3. Apparently the present simulation captures the trend of this phenomenon well.

3. DISLOCATION EVOLUTION IN EPITAXIAL MULTILAYERS AND GRADED BUFFERS

For epitaxial multilayers, threading dislocations can bend over to any interface within the structure. Let ρ_i be the dislocation density of the i th threading dislocations, which begin on the free surface, thread across the thickness and bend to the i th interface. Figure 4 shows a schematic diagram of the epitaxial multilayers. Let the i th layer have a misfit strain with

respect to the substrate of ϵ_{0i} , and a thickness w_i . For the i th layer, we have following evolution equations:

$$\dot{\epsilon}_{pi} - \dot{\epsilon}_{pi-1} = \rho_i b_1 v_i / 2, \quad (14)$$

$$v_i = v_0 \left(\frac{\tau_{\text{exci}} - \tau_{Ri}}{\mu} \right)^m \exp\left(-\frac{Q_v}{kT}\right), \quad (15)$$

$$\dot{\rho}_i = (\dot{\rho}_i)_{\text{nucl}} - (\dot{\rho}_i)_{\text{annih}}, \quad (16)$$

$$(\dot{\rho}_i)_{\text{annih}} = \eta_0 \rho_i v_i / p_i \quad (17)$$

and

$$(\dot{\rho}_{\text{tot}})_{\text{nucl}} = \xi_0 \left(\frac{\tau - \tau_0 - \tau_R}{\mu} \right)_{\text{top}}^n \exp\left(-\frac{Q_p}{kT}\right), \quad (18)$$

where $\dot{\epsilon}_{pi}$ is the plastic strain rate of the i th layer, v_i is the average velocity of the i th threading dislocations, τ_{Ri} is the corresponding resistance arising from dislocation interactions, τ_{exci} is the average excess stress acting on the i th threading dislocations, p_i is the average spacing of the i th misfit dislocations in the i th interface. Equation (18) considers only the nucleation rate of total threading dislocation. The subscript “top” denotes that the corresponding quantities belong to the top layer. The total nucleated threading dislocations are distributed to all layers according to an unknown weight. The power function of the i th effective stress, $\tau_{\text{effi}} = \tau_{\text{exci}} - \tau_{Ri}$, may be the simplest weight. Then we have

$$(\dot{\rho}_i)_{\text{nucl}} = (\dot{\rho}_{\text{tot}})_{\text{nucl}} \left(\frac{\tau_{\text{effi}}}{\mu} \right)^n / S, \quad (19)$$

where

$$S = \sum_{i=1}^N \left(\frac{\tau_{\text{effi}}}{\mu} \right)^n, \quad (20)$$

N being the total number of layers in the epitaxial multilayers. It is worth noting that equation (18) is suitable only for the case of $S > 0$, otherwise $(\dot{\rho}_{\text{tot}})_{\text{nucl}}$ should be equal to zero.

The effective stress τ_{effi} acting on the i th threading dislocations can be expressed as

$$\tau_{\text{effi}} = c\mu \left\{ \sum_{j=1}^N w_j [\epsilon_{0j} - \epsilon_{pj} - H(\epsilon_{pj})] - \Gamma b \ln\left(\frac{2h_i}{b}\right) \right\} / h_i, \quad (21)$$

where h_i is the depth from the free surface to the i th interface. From equation (14), one can easily obtain the following formulas

$$\epsilon_{pi} = b_1 \sum_{j=1}^i \rho_j v_j / 2 \quad (22)$$

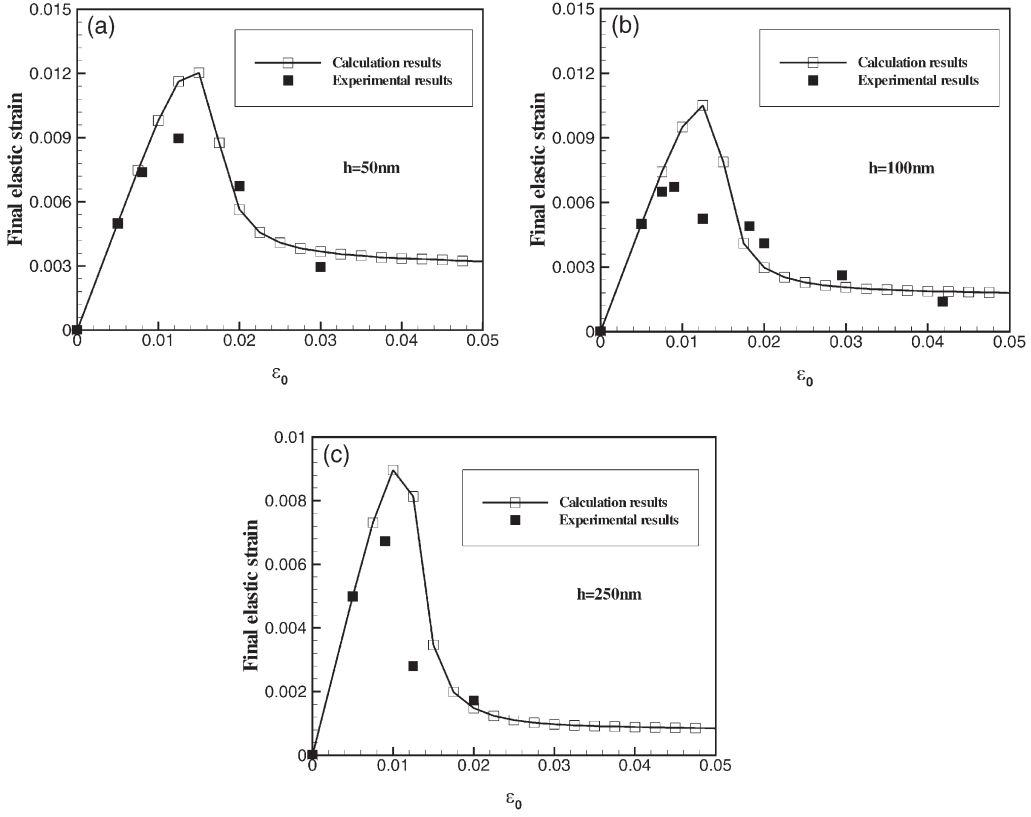


Fig. 3. Final elastic strain versus initial mismatch strain following growth of the $\text{Ge}_x\text{Si}_{1-x}/\text{Si}(100)$ material system at 550°C : (a) $h = 50$ nm, (b) $h = 100$ nm, (c) $h = 250$ nm. The experimental data (filled points) were given by Bean *et al.* [12] for a growth rate of 0.5 nm s^{-1} . All unfilled points are the present calculation results.

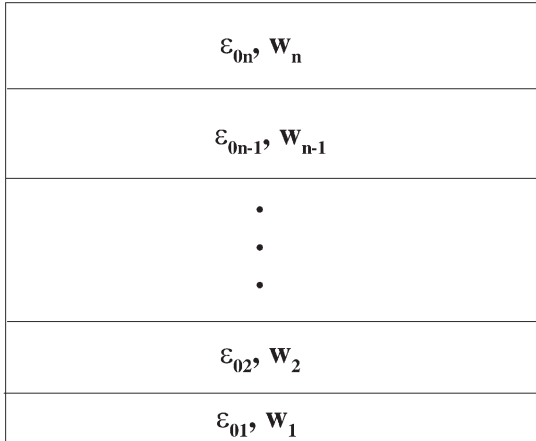


Fig. 4. Schematic cross-section of an epitaxial multilayer system.

and

$$\kappa_i = \rho_i v_i / 2, \quad (23)$$

where κ_i is the linear density of the misfit dislocations at the i th interface.

The composition graded buffer can be treated as an epitaxial multilayer. For a linear graded buffer in the

$\text{Ge}_x\text{Si}_{1-x}/\text{Si}$ material system, the misfit strain of the i th layer, ε_{0i} , is

$$\varepsilon_{0i} = 0.0418 R_g z_i, \quad (24)$$

where R_g is the composition grading rate, and z_i is the height of the i th interface from the bottom of the epitaxial multilayer system.

Fitzgerald *et al.* [9] have grown compositionally graded $\text{Ge}_x\text{Si}_{1-x}$ on Si. The growth temperature was typically $700\text{--}900^\circ\text{C}$ and the growth rate was 3 \AA s^{-1} . For each sample, a $1 \mu\text{m}$ uniform-composition cap layer was grown after the graded buffer. The final Ge concentrations of three samples were 24%, 32% and 50%. The threading dislocation densities measured for them were $4.4 \times 10^5 \pm 5 \times 10^4$, $1.7 \times 10^6 \pm 1.5 \times 10^5$ and $3.0 \times 10^6 \pm 2 \times 10^6 \text{ cm}^{-2}$, respectively.

Fitzgerald *et al.* [9] investigated the effect of grading rate on the threading dislocation density. They found that the threading dislocation densities were relatively insensitive to grading rate. In order to save the computation cost, we chose a large Ge grading rate instead of the experimental grading rate of 10% Ge per μm . In the present simulations, the thickness of the graded buffer layers is chosen to be 500 nm and the total thickness to be $h = 1.5 \mu\text{m}$. The total number of layers N for the buffer is 500 . The Ge grad-

ing rate used by the present simulation is $R_g = 2x_{\max} \mu\text{m}^{-1}$.

The trapezoid integration rule is used in the calculation. The total number of integration steps for each of the three samples is 30×10^4 . A comparison of experimental data and the present simulation is shown in Table 1, which shows clearly that the present simulations agree well with the measured results.

The major advantage in using the graded composition buffer is that instead of the misfit dislocations being bent to a single interface, there will be a distribution through the buffer layer. This provides more freedom for misfit dislocations to propagate past each other as they will be at different heights in the structure, thereby minimizing pinning events. Meanwhile this also provides more opportunity for threading dislocation annihilations, since the annihilation can occur not only between dislocations within the same layer but also between different layers. Hence the empirical formula (10) does not seem to be suitable for epitaxial multilayers and graded composition buffers. In the present simulation for epitaxial multilayers and graded composition buffers, the parameter η_0 is simply taken to be constant for each sample.

Figure 5 reveals the evolution of the threading dislocation density with the increase of plastic strain at the surface. At the beginning, the threading dislocation density increases monotonically as the plastic strain at the surface increases during growth of the graded buffer. The process is dominated by threading dislocation nucleation. After growth of the graded buffer, the effective stress τ_{eff} gradually approaches zero and the threading dislocation nucleation rate becomes less than the threading dislocation annihilation rate. Therefore the threading dislocation density decreases with the plastic strain increase. The transition occurs slowly, and consequently there seems to be a steady state in the interval $\epsilon_p = (0.0003, 0.0006)$ for sample A. For sample C, a quasi-steady state appears in the interval $\epsilon_p = (0.002, 0.016)$.

The evolution of the threading dislocation density versus growth height is shown in Fig. 6. It can be seen that the threading dislocation density increases monotonically as the growth height increases during growth of the graded buffer. The threading dislocation density arrives first at a quasi-saturation state,

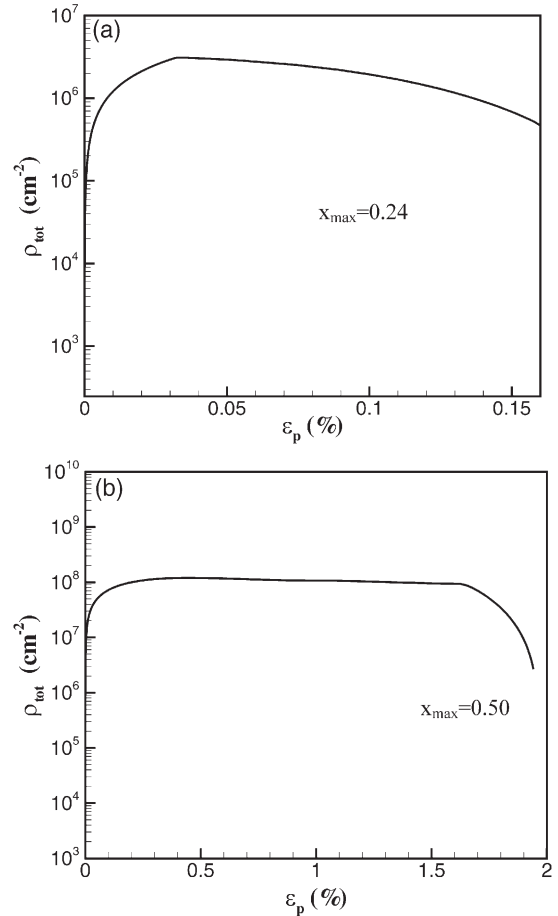


Fig. 5. Total threading dislocation density, ρ_{tot} , versus relaxed plastic strain of top layer, ϵ_p , during growth of a $\text{Ge}_x\text{Si}_{1-x}/\text{Si}(100)$ graded buffer on Si and post-growth of a 1 μm uniform-composition cap on the buffer for 24% Ge (a) and 50% Ge (b) samples.

and then decreases monotonically as the growth height increases further during growth of a uniform cap layer.

4. CONCLUSIONS

In this paper we have proposed models to describe the dislocation dynamics of strain relaxation in an epitaxial uniform layer, epitaxial multilayers and

Table 1. The comparison of experimental data and present simulation data

| | Sample A | Sample B | Sample C |
|--------------------------------------------------------------|-------------------------------------|---------------------------------------|-------------------------------------|
| Final Ge composition (%) | 24 | 32 | 50 |
| Simulation grading rate, $\text{Ge } \mu\text{m}^{-1}$ (%) | 48 | 64 | 100 |
| Experimental temperature ($^{\circ}\text{C}$) | 700–900 | 700–900 | 700–900 |
| Simulation temperature ($^{\circ}\text{C}$) | 700 | 700 | 700 |
| Measured threading dislocation density (cm^{-2}) | $4.4 \times 10^5 \pm 5 \times 10^4$ | $1.7 \times 10^6 \pm 1.5 \times 10^5$ | $3.0 \times 10^6 \pm 2 \times 10^6$ |
| η_0 | 0.12 | 0.06 | 0.25 |
| Simulated threading dislocation density (cm^{-2}) | 4.71×10^5 | 1.31×10^6 | 2.66×10^6 |

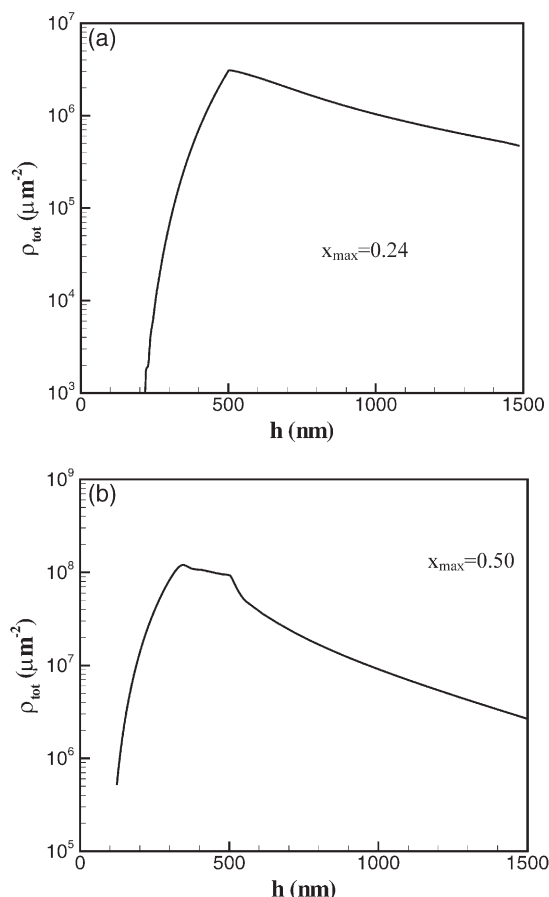


Fig. 6. Total threading dislocation density, ρ_{tot} , versus growth height, h , during growth of a $\text{Ge}_x\text{Si}_{1-x}/\text{Si}(100)$ graded buffer on Si and post-growth of a $1\ \mu\text{m}$ uniform-composition cap on the buffer for 24% Ge (a) and 50% Ge (b) samples.

graded composition buffers. The model for a single epitaxial layer consists of five evolution equations. The first equation is the plastic strain rate equation. The second equation denotes the mean velocity of the threading dislocations, in which a resistance term τ_R is introduced to consider dislocation interactions. The dislocation interactions are assumed to depend only on the plastic strain. Both threading dislocation nucleation and annihilation are considered in the last three evolution equations. The dislocation nucleation is closely related to the coherency stress in the layer.

Besides the resistance force τ_R , we also introduce a threshold stress τ_0 in the nucleation rate equation of the threading dislocations. The dislocation annihilation rate equation is established based on an ideal periodical array of rectangular cells and then modified through the effective factor η_0 . The present simulation reveals that the parameter η_0 , which may depend on fabrication process and surface morphology, is vital for achieving low threading dislocation density. Then the evolution equations are extended to epitaxial multilayers and graded buffers. The evolution equations successfully predict a wide range of experimental results on strain relaxation and threading dislocation evolutions in $\text{Ge}_x\text{Si}_{1-x}/\text{Si}(100)$ heterostructures. Meanwhile, the simulation results show clearly that promoting annihilation of threading dislocations is very effective in the process of threading dislocation reductions.

Acknowledgements—T.C.W. wishes to acknowledge financial support by The National University of Singapore, where he spent his sabbatical leave.

REFERENCES

1. Liu, W. K. and Santos, M. B., *Thin Films: Heteroepitaxial Systems*. World Scientific Publishing, London, 1999.
2. Tsao, J. Y., *Materials Fundamentals of Molecular Beam Epitaxy*. Academic Press, Boston, MA, 1993.
3. Fitzgerald, E. A., Kim, A. Y., Currie, M. T., Langdo, T. A., Taraschi, G. and Bulsara, M. T., *Mater. Sci. Eng. B*, 1999, **67**, 53.
4. Fitzgerald, E. A., Currie, M. T., Samavedam, S. B., Langdo, T. A., Taraschi, G., Yang, V., Leitz, C. W. and Bulsara, M. T., *Phys. Stat. Sol.*, 1999, **171**, 227.
5. Dodson, B. W. and Tsao, J. Y., *Appl. Phys. Lett.*, 1987, **51**, 1325.
6. Hull, R., Bean, J. C. and Buescher, B., *J. Appl. Phys.*, 1989, **66**, 5837.
7. Houghton, D. C., *J. Appl. Phys.*, 1991, **70**, 2136.
8. Gosling, T. J., Jian, S. C. and Harker, A. H., *Phys. Stat. Sol. (a)*, 1994, **146**, 713.
9. Fitzgerald, E. A., Xie, Y. H., Monroe, D., Silverman, P. J., Kuo, J. M., Kortan, A. R., Thiel, F. A. and Weir, B. E., *J. Vac. Sci. Technol. B*, 1992, **10**, 1807.
10. Romanov, A. E., Pompe, W., Mathis, S., Beltz, G. E. and Speck, J. S., *J. Appl. Phys.*, 1999, **85**, 182.
11. Orowan, E., *Proc. Phys. Soc.*, 1940, **52**, 8.
12. Bean, J. C., Feldman, L. G., Fiory, A. T., Nakahara, S. and Robinson, I. K., *J. Vac. Sci. Technol. A*, 1984, **2**, 436.
13. Freund, L. B., in *Advances of Applied Mechanics*. Academy Press, San Diego, 1994, Vol. 30, p. 1.